Journal of Hazardous Materials 170 (2009) 1064–1069

Contents lists available at ScienceDirect

Journal of Hazardous Materials

journal homepage: www.elsevier.com/locate/jhazmat

Removal of azobenzene from water by kaolinite

Xiaoling Zhang [a], Hanlie Hong [a], Zhaohui Li [b,c,*], Junfang Guan [d], Laura Schulz [b]

[a] The Faculty of Earth Sciences, China University of Geosciences, Wuhan, Hubei 430074, China
[b] Department of Geosciences, University of Wisconsin-Parkside, 900 Wood Road, Kenosha, WI 53144, USA
[c] Department of Earth Sciences, National Cheng Kung University, 1 University Road, Tainan 70101, Taiwan
[d] School of Resource & Environmental Engineering, Wuhan University of Technology, Wuhan, Hubei 430070, China

ARTICLE INFO

Article history:
Received 15 January 2009
Received in revised form 14 April 2009
Accepted 18 May 2009
Available online 22 May 2009

Keywords:
Azobenzene
Adsorption
Isotherm
Kaolinite
Kinetics

ABSTRACT

The use of natural kaolinite clay to remove azobenzene from aqueous solutions under different pHs, ionic strengths, initial solid mass used, and initial solution concentrations was investigated. Batch kinetic experiments showed that the adsorption of azobenzene onto kaolinite followed a pseudo-second-order kinetics with an initial rate of 7.2 mg/g-h and a rate constant of 0.19 g/mg-h. The equilibrium azobenzene adsorption on kaolinite was well described by the Langmuir and Freundlich isotherms with an adsorption capacity of 11 mg/g, or 60 mmol/kg, corresponding to a monolayer adsorption on the surface of kaolinite. Adsorption increased with decreases in solution pH and increases in solution ionic strength. The enthalpy change of adsorption was −38 kJ/mol, suggesting that both physical and chemical adsorption was responsible for the retention of azobenzene on kaolinite. The high affinity of azobenzene for siloxane and gibbsite surfaces was attributed to the attractive Coulombic and van der Waals' forces between the surface and the planar structure of the organic molecule.

1. Introduction

Many dyes and pigments are toxic and have carcinogenic and mutagenic effects that affect aquatic biota as well as humans [1]. Azo dyes constitute a family of dyes and make up 60–70% of all textile dyestuffs [2]. Wide use of azo dyes in China resulted in elevated concentration in water and soil [3]. Azobenzene ($C_{12}H_{10}N_2$) is one of the common components of azo dyes, and is also a decomposition product of many aniline-based herbicides [4].

Common techniques to remove azo dyes from water include biological [2], photocatalytic [5], and physical treatments [6]. In addition, sorptive removal using low cost adsorbents has also been investigated in great details [7–10]. Clay minerals have large specific surface area and high cation exchange capacity (CEC), and have been extensively studied for potential applications as environmental remediation agents to remove heavy metals and organic contaminants from water [11]. Studies on sorptive removal of azo dyes using native materials were mainly focused on basic dyes as they are often in cationic form while clay minerals bear negative charges on their surfaces [3,7–10,12]. Acidic dyes in anionic form could be removed by clay minerals after surfactant modification that reversed the surface charge to positive [6,13].

Kaolinite is one of the most common clay minerals found on the surface of the Earth. For the past few decades kaolinite has been tested on the adsorption of organic complexes as well as azo dyes [14–16]. Adsorption and ion exchange would result in decolorization of dyes [17], which could also be influenced by many physio-chemical factors, such as, dye/sorbent interaction, sorbent surface area, particle size, temperature, pH, and contact time [18].

In this research, we studied the removal of azobenzene, the basic component of azo dyes, by kaolinite as a function of pH, ionic strengths, temperature, and initial azobenzene to kaolinite ratio at a batch scale, followed by discussions on mechanisms of adsorption onto kaolinite.

2. Experimental

2.1. Materials

Kaolinite belongs to phyllosilicates made of one layer of tetrahedral sheets and one layer of octahedral sheets. Siloxane and gibbsite surfaces make up the external surfaces of the tetrahedral and octahedral sheets, respectively. These surfaces could interact with different functional groups resulting in adsorption of organic molecules on the surfaces.

The kaolinite used in this study was obtained from Maoming, Guangdong, China. XRD and IR measurements showed very high purity with only trace amount of feldspar. The mean particle size of aggregates was 4.5 μm with a uniformity coefficient of 8 for the

* Corresponding author at: Department of Geosciences, University of Wisconsin-Parkside, 900 Wood Road, Kenosha, WI 53144, USA. Tel.: +1 262 595 2487; fax: +1 262 595 2056.
E-mail address: li@uwp.edu (Z. Li).

0304-3894/$ – see front matter © 2009 Elsevier B.V. All rights reserved.
doi:10.1016/j.jhazmat.2009.05.073

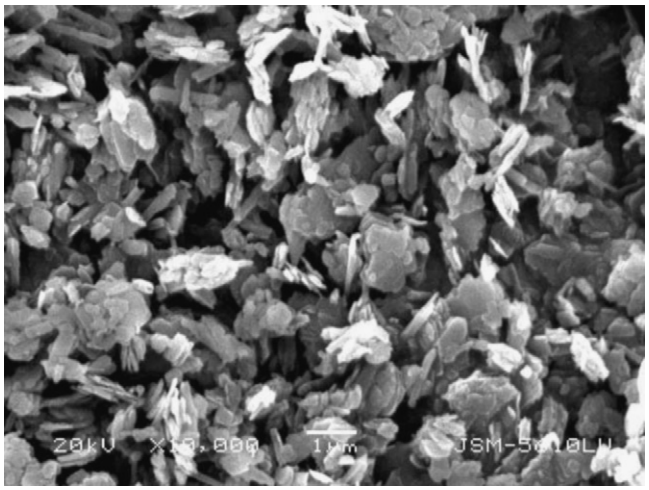

Fig. 1. SEM photo showing the crystal size of kaolinite used in this study.

raw kaolinite determined by a hydrometer method. The individual grain size as observed by SEM is about 1 μm for larger particles and 0.3 μm for small ones with an average thickness of 0.1 μm (Fig. 1). The specific surface area (SSA) is 28–30 m^2/g while the CEC is 3.6–3.8 cmol/kg measured by a spot methylene blue method [19]. A comparison between this method and the conventional BET method for SSA and titration method for CEC determinations provided good agreements [20] and the method is currently listed as a standard method for laboratory analysis of bentonite in UK [21].

The azobenzene was purchased from Sinopharm Chemical Reagent Co. Ltd. (Shanghai, China). Its chemical formula is $C_{12}H_{10}N_2$ and structure is illustrated in Fig. 2.

2.2. Batch kinetic study

To each 100 mL centrifuge tube, 0.25 g of kaolinite and 50 mL of azobenzene solution at 50 mg/L were mixed on a reciprocal shaker at 150 rpm for 0.25, 0.5, 1.0, 2.0, 4.0, 8.0, and 24.0 h at pH 7. Due to the low solubility of azobenzene, it was first dissolved in ethanol before aqueous solutions with targeted initial concentrations were made. The tubes were wrapped with aluminum foils to prevent light induced decomposition during mixing and storage processes. At the end of each time, the samples were centrifuged for 20 min at 4000 rpm and the supernatant analyzed immediately for equilibrium azobenzene concentrations by a spectrophotometric method. The amount of azobenzene adsorbed was determined by the difference between the initial and equilibrium concentrations.

2.3. Adsorption studies

To each 100 mL centrifuge tube, 0.25 g of kaolinite and 50 mL of azobenzene solution at concentrations of 10, 30, 50, 70, 90, and 100 mg/L were added. The pH of each suspension was adjusted to a desired value with additions of dilute HCl or NaOH solution. The ionic strength was adjusted by adding NaCl to desired concentrations. For thermodynamic study, the temperature was controlled at 288 K, 313 K and 333 K. The mixtures were shaken in a thermostatic shaker bath at 25 °C for 24 h. After the contact time was completed, the suspension was centrifuged at 4000 rpm for 20 min. Azobenzene remaining in the supernatant was analyzed by the spectrophotometric method. The amount of azobenzene adsorbed was determined by the difference between the initial and equilibrium concentrations. A control experiment was performed in the absence of kaolinite to evaluate the loss of azobenzene due to adsorption on glassware at all input concentrations. A decrease about 10% of the original concentration was noticed and corrections were made for such decrease. All assays were carried out in duplicate.

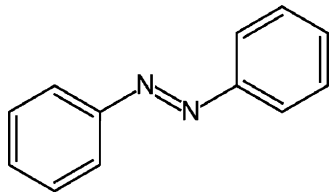

Fig. 2. Molecular structure of azobenzene.

2.4. Methods of analyses

The azobenzene concentration was analyzed by a UV–vis spectrophotometer at the wavelength of 320 nm. The spectrum bandwidth was 6 nm with a precision of ±2 nm. Transmittance accuracy was ±1.5%. Stray light was ≤0.7% (t) at 320 nm. Calibrations with the six initial concentrations resulted in a coefficient of determination r^2 of 0.997.

Powder XRD analysis was performed on a Rigaku D/Max-IIIa diffractometer with Ni-filtered Cu Kα radiation at 35 kV and 35 mA. XRD patterns of randomly oriented samples were collected from 2° to 65° 2θ at a scanning rate of 2° min^{-1}.

FTIR analysis was undertaken on a Nicolet 60 SXB Fourier transform infrared spectrometer. The spectra were recorded in the region from 400 to 4000 cm^{-1} with a spectral resolution of 2 cm^{-1}, using a pressed KBr pellet technique.

3. Result and discussion

3.1. Azobenzene adsorption kinetics

Kinetics of azobenzene adsorption on kaolinite is presented in Fig. 3. The data were fitted to several kinetic models. The pseudo-second-order kinetic model takes the form [22]:

$$\frac{dq_e}{dt} = \frac{k_2}{(q_e - q_t)^2} \quad (1)$$

Its linear integrated form is

$$\frac{t}{q_t} = \frac{1}{k_2 q_e^2} + \frac{1}{q_e} t \quad (2)$$

where q_e and q_t are the solute adsorbed at equilibrium and at time t (mg/g), k_2 (g/mg-h) is the rate constant of the pseudo-second-order adsorption, while $k_2 q_e^2$ is the initial rate (mg/g-h). When the

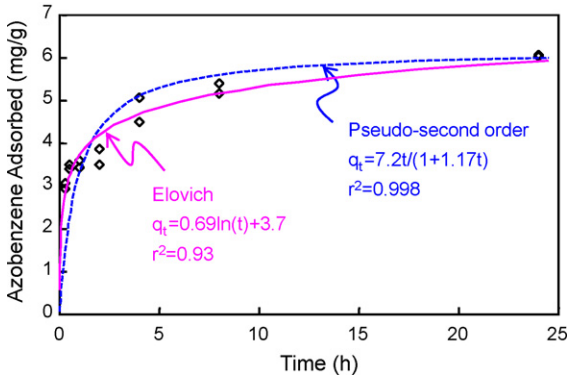

Fig. 3. Kinetics of azobenzene adsorption on kaolinite fitted to pseudo-second-order and Elovich models.

kinetic data were fitted to Eq. (2), the r^2 was 0.998, the initial rate was 7.2 mg/g-h, the rate constant was 0.19 g/mg-h, and the q_e was 6.2 mg/g.

The Elovich model can be written as [23]

$$q_t = a\ln(t) + b \tag{3}$$

where a and b are constants, whose fitted values were 0.69 mg/g-h and 3.7 mg/g, respectively, with an r^2 of 0.93. Compared to the Elovich model, the pseudo-second-order kinetic model described the azobenzene adsorption better. The pseudo-second-order kinetics achieved a much large r^2 compared to pseudo-first-order kinetics for adsorption of Azo Dye C.I. Acid Red 14 on soils [12] and that of Congo Red on surfactant-modified montmorillonite (SMM) [13]. The rate constant from this study is 3–5 times faster than that for the adsorption of Azo Dye C.I. Acid Red 14 on soil [12] and 6 times faster than that for the adsorption of Congo Red onto SMM [13]. The pseudo-first-order kinetics did not fit the data as nicely as the pseudo-second-order one. Thus, it was excluded from discussion here. Fig. 3 also showed that equilibrium could be reached in 24 h. Thus, the equilibration time was set at 24 h for other adsorption tests.

3.2. Azobenzene adsorption isotherm

The adsorption data were fitted to the Langmuir and Freundlich isotherms. The former takes the form of

$$C_S = \frac{K_L S_m C_L}{1 + K_L C_L} \tag{4}$$

where C_S is the amount of solute adsorbed on solid at equilibrium (mg/g), C_L the equilibrium solute concentration (mg/L), S_m the apparent adsorption capacity or adsorption maximum (mg/g), and K_L the Langmuir coefficient (L/mg). Eq. (4) can be rearranged to a linear form

$$\frac{C_L}{C_S} = \frac{1}{K_L S_m} + \frac{C_L}{S_m} \tag{5}$$

so that K_L and S_m can be determined by a linear regression. The coefficient of determination r^2 is 0.98 and the calculated S_m is 11 mg/g, or 60 mmol/kg, and K_L is 0.05 L/mg for azobenzene adsorption on kaolinite. Knowing the azobenzene adsorption capacity and the SSA, the area occupied per molecule could be determined by $\Phi = (10^{20}/\Gamma_{\max} A)$SSA Å/molecule [6], where $\Gamma_{\max}$ is the solute adsorption maximum and A is the Avogadro's constant. Using the SSA of 28–30 m^2/g determined from the methylene blue method and the azobenzene adsorption capacity determined from the isotherm test, the calculated area occupied per azobenzene molecule was 77–83 $Å^2$, compared to an all *trans*-conformation of 68 $Å^2$ [24]. At all *cis*-conformation, the azobenzene molecule would have a cross section area of 50 $Å^2$ [24]. When adsorbed to Cu(1 1 0) surface, the dimension of azobenzene was restricted by the surface arrangement of Cu atoms, resulting in a dimension of 112 $Å^2$ with all *trans*-conformation [25]. It seems that at the azobenzene adsorption maximum, the adsorbed molecules would take all *trans*-conformation with a monolayer sorption, which justified the use of Langmuir sorption isotherm (Fig. 4).

The Freundlich isotherm has the form of

$$C_S = K_F C_L^{1/n} \tag{6}$$

where K_F and n are constants. Eq. (6) can be rearranged to a linear form

$$\ln\ C_S = \frac{1}{n}\ln C_L + \ln K_F \tag{7}$$

The regression coefficient r^2 is 0.95 and the values of n and K_F are 0.6 and 1 L/g. Similar to Langmuir isotherm, Freundlich isotherm described the adsorption of azobenzene on kaolinite equally well in terms of r^2 (Fig. 4).

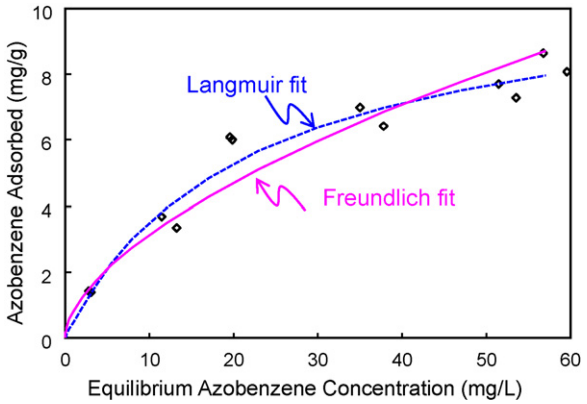

Fig. 4. Adsorption of azobenzene on kaolinite fitted to the Langmuir and Freundlich isotherms.

Langmuir isotherm was found better describing adsorptions of Congo Red on SMM [13], and anionic dyes naphthol red-J and direct orange on nontronite [10]. On the contrary, Freundlich isotherm fitted the data better than Langmuir isotherm for the adsorption of Azo Dye C.I. Acid Red 14 on soil [12]. However, both Langmuir and Freundlich isotherms fit the data equally well for adsorption of methylene blue with a monolayer coverage on kaolinite [14]. The adsorption capacity of azobenzene on kaolinite in this study is much higher than that of Azo Dye C.I. Acid Red 14 on soil [12], comparable to that of neutral azo dye C.I. Vat Yellow 2 on natural sediments in Qinghe River [3], lower than that of anionic dyes on natural sediments in Qinghe River [3], and much lower than that of Congo Red, also an anionic dye, on SMM [13]. As azobenzene is hydrophobic, its adsorption could be predominantly by hydrophobic bonding in contrast to electrostatic interaction between ionic dyes and charged mineral surfaces.

3.3. Effect of pH on azobenzene adsorption

Azobenzene has a p*K*a value of 3.3 while the point of zero charge (pzc) of kaolinite is about 4 [26]. Lower pH facilitated adsorption of azobenzene while higher pH prohibited adsorption of azobenzene on kaolinite (Fig. 5). A similar pH effect was observed for adsorption of some azo dyes on nontronite [10] and of C.I. Acid Red 14 on selected soils collected from Germany and China [12]. A slight increase in adsorption of cationic dyes and a drastic decrease in adsorption of anionic dye were found on surface sediments from Qingher River in Beijing, China [3]. At the pH lower than the p*K*a of azobenzene and pzc of kaolinite, kaolinite is positively charged

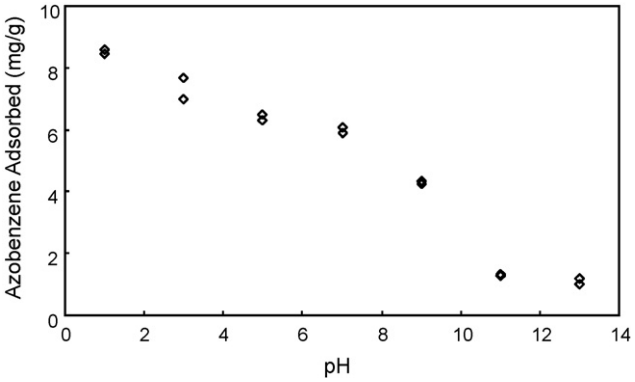

Fig. 5. Influence of solution pH on azobenzene adsorption.

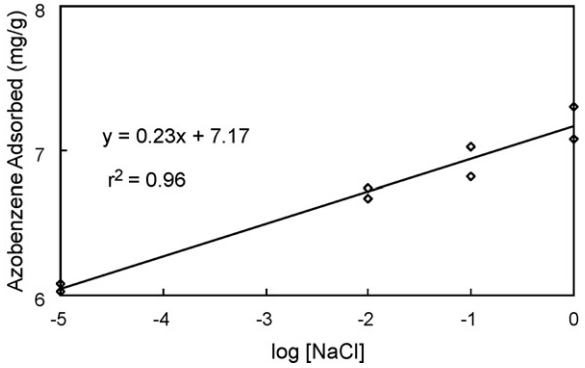

Fig. 6. Influence of ionic strength on azobenzene adsorption.

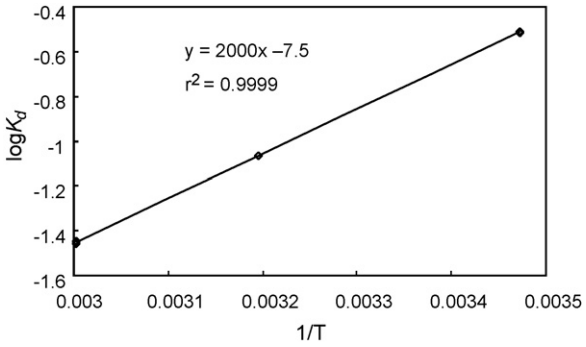

Fig. 8. Linear relation between $\log K_d$ and $1/T$.

while azobenzene exists as neutral molecule. The higher adsorption of azobenzene could be attributed to hydrophobic interaction. The lone pair electrons on the nitrogen may be attracted to the positively charged kaolinite surfaces at the pHs less that the pzc, or even less than the p*K*a of azobenzene, resulting in a higher azobenzene adsorption and retention. As solution pH increased beyond the pzc of kaolinite, the surface will become progressively negatively charges while the dissociation of azobenzene into negatively charged species prevented their adsorption on kaolinite surfaces. In contrast, for cationic dye methylene blue, an increase in adsorption was accompanied by an increase in pH [14].

3.4. Effect of ionic strength on azobenzene adsorption

Industrial dyeing-wastewater usually has high inorganic salt level [27]. Thus, it is necessary to investigate the effect of dissolved salts on the adsorption of azobenzene on kaolinite. An increase in azobenzene adsorption is accompanied by an increase in ionic strength as represented by NaCl (Fig. 6). A similar observation was found for adsorption of C.I. Acid Red 14 on selected soils collected from Germany and China [12]. However, a reverse trend was also observed for adsorption of basic dyes onto sediments from Qinghe River [3]. A higher ionic strength would reduce the double layer thickness and result in a stronger interaction between the hydrophobic sorbate and the sorbent.

3.5. Effect of initial kaolinite mass on azobenzene adsorption

The influence of initial kaolinite mass on azobenzene adsorption is illustrated in Fig. 7. At an initial azobenzene concentration of 50 mg/L, a higher initial kaolinite mass resulted in a lower amount adsorbed per unit mass. The inflection point of the curve is at the kaolinite to solution ratio between 4 and 10 g/L, which was the justification of the solid to liquid ratio of 0.25 g to 50 mL used for the batch tests.

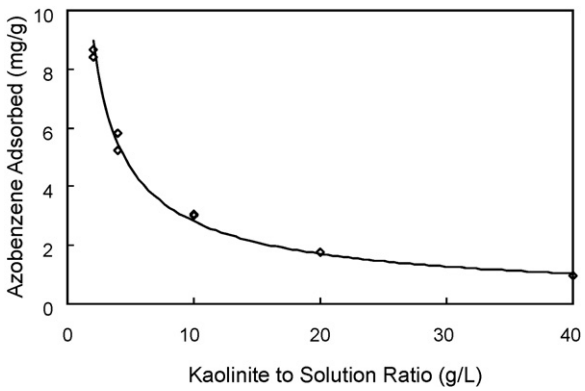

Fig. 7. Influence of solid to liquid ratio on azobenzene adsorption.

3.6. Effect of temperature on azobenzene adsorption

The temperature effect on azobenzene adsorption is expressed by

$$\log\ K_d = -\frac{\Delta H}{2.303RT} + \frac{\Delta S}{R} \quad (8)$$

where K_d is the distribution coefficient of azobenzene between the solid and the liquid phases, ΔH is the change in enthalpy, ΔS is the charge in entropy, R is the gas constant, and T is the reaction temperature in K. A plot of $\log K_d$ against $1/T$ revealed a linear relationship (Fig. 8), with a ΔH value of −38 kJ/mol and ΔS of −62 J/mol K. The

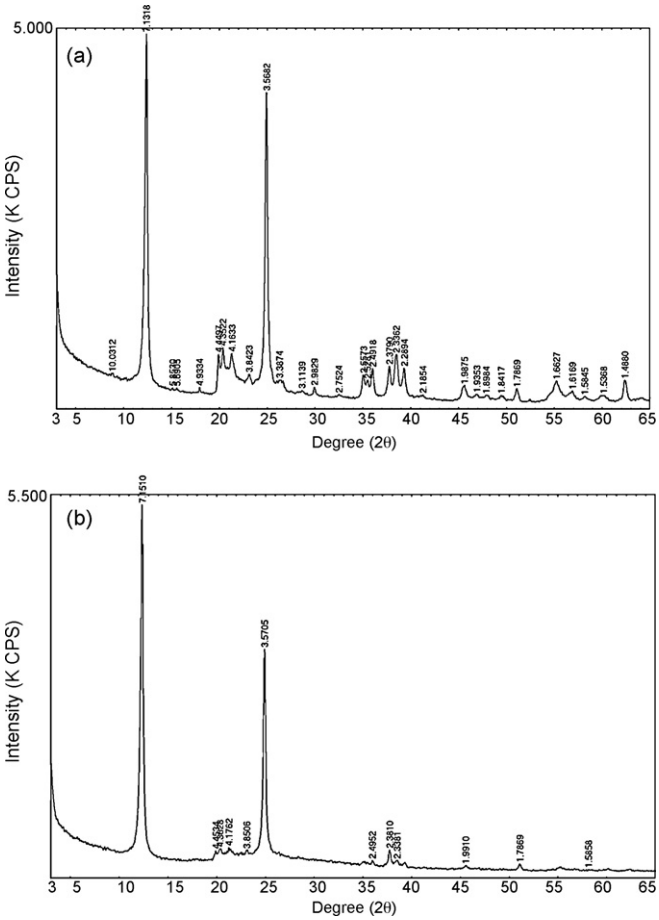

Fig. 9. XRD patterns of kaolinite (a) and azobenzene-adsorbed kaolinite (b).

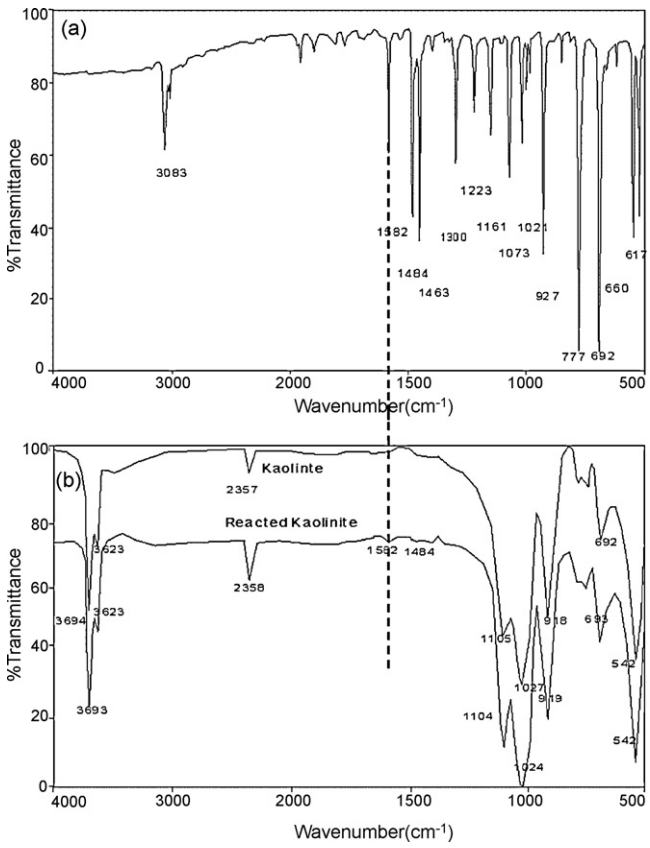

Fig. 10. FTIR spectra showing the band positions of azobenzene (a) and kaolinite and azobenzene-adsorbed kaolinite (b).

negative ΔH value suggested that azobenzene adsorption was an exothermal process and therefore decreases in temperature should facilitate its adsorption onto kaolinite. The ΔH value could be used to distinguish physical from chemical adsorption with a borderline at −40 kJ/mol. The ΔH value of −38 kJ/mol suggested that both physical and chemical adsorption were equal important in azobenzene retention with the former corresponding to hydrophobic and electrostatic interactions while the letter to surface complexation. The observation was consistent to the study of Plemenschikov and Leszczyski [28] that a high affinity of 1,3,5-trinitrobenzene for a model siloxane surface was attributed to the attractive Coulombic and van der Waals' forces between the surface and the planar structure of organic molecule.

The change in free energy ΔG after azobenzene adsorption can be calculated from

$$\Delta G = \Delta H - T\,\Delta S \quad (9)$$

The calculated ΔG is −20 kJ/mol (at 25 °C). The ΔG values from this study are more negative compared to those for methylene blue adsorption on kaolinite [14], for naphthol red-J and direct orange dyes adsorption on nontronite [10], and much negative for C.I. Acid Red 14 adsorption on selected soils [12]. The negative ΔG value indicates attractive interaction between azobenzene and kaolinite.

3.7. XRD analysis

The XRD pattern (Fig. 9) of the purified sample showed a pure kaolinite. After equilibrated with azobenzene for 24 h, the XRD pattern did not change at all, suggesting that the adsorption took place mainly on the external surface of kaolinite, in contrast to intercalation of benzaminde in kaolinite [29], nitroaniline in kaolinite [30], and cyclic imides in kaolinite [31].

3.8. FTIR analysis

The infrared spectra of kaolinite and azobenzene-adsorbed kaolinite are shown in Fig. 10. The suggested peak assignments were compared to the published results [29,31,32]. The bands associated with the ν(C–C) stretching vibrations of the phenyl rings are located at 1484 and 1582 cm^{-1} [33,34]. The main band positions for Si–O, Si–O–Si, Al–O, and Al–O–Al had not distinctly shifted, indicating that the high affinity of azobenzene for siloxane and gibbsite surfaces was attributed to the attractive Coulombic and van der Waals' forces between the surface and the planar structure of organic molecules, which is consistent with previous results [28,35].

4. Conclusions

The removal azobenzene from water by kaolinite was systematically investigated under various conditions. The adsorption of azobenzene on kaolinite increased with the decrease of pH and increase of the NaCl concentration. Kinetics of azobenzene adsorption onto kaolinite fit to the pseudo-second-order model well. Both Langmuir and Freundlich isotherms described azobenzene adsorption equally well with an adsorption capacity as high as 11 mg/g, or 60 mmol/gk, corresponding to a monolayer adsorption on the surface of kaolinite. The enthalpy change (ΔH) is −38 kJ/mol, suggesting both chemical and physical sorption was important for retention of azobenzene on kaolinite. XRD and FTIR analyses show no significant change in peak positions, suggesting that affinity of azobenzene for siloxane and gibbsite surfaces was attributed to the attractive Coulombic and van der Waals' forces between the surface and the planar structure of organic molecules without any intercalation.

Acknowledgments

The research is supported by the Key Project of Chinese Ministry of Education (107076) and partially supported by a funding from Wisconsin Groundwater Research Council. Funding from National Cheng Kung University (NCKU) for the project of Promoting Academic Excellence & Developing World Class Research Center to support Li as visiting professor in NCKU made this publication possible. We thank the anonymous reviewers for their constructive comments to improve the quality of the manuscript.

References

[1] G. McKay, M.S. Otterburn, D.A. Aga, Fullers earth and fired clay as adsorbent for dye stuffs. Equilibrium and rate constants, Water Air Soil Pollut. 24 (1985) 307–322.
[2] C.M. Carliell, S.J. Barclay, C.A. Buckley, Treatment of exhausted reactive dye bath effluent using anaerobic digestion: laboratory and full scale trials, Water SA 22 (1996) 225–233.
[3] R.X. Liu, X.M. Liu, H.G. Tang, Y. Su, Sorption behavior of dye compounds onto natural sediment of Qinghe River, J. Colloid Interface Sci. 239 (2001) 475–482.
[4] L.M. Bordeleau, R. Bartha, Azobenzene residues from aniline-based herbicides; evidence for labile intermediates, Bull. Environ. Contam. Toxicol. 5 (1970) 34–37.
[5] A. Akyol, M. Bayramoglu, The degradation of an azo dye in a batch slurry photocatalytic reactor, Chem. Eng. Process. 47 (2008) 2150–2156.
[6] Y.E. Benkli, M.F. Can, M. Turan, M.S. Celik, Modification of organo-zeolite surface for the removal of reactive azo dyes in fixed-bed reactors, Water Res. 39 (2005) 487–493.
[7] V.K. Gupta, I. Ali, Suhas, D. Mohan, Equilibrium uptake and sorption dynamics for the removal of a basic dye (basic red) using low cost adsorbents, J. Colloid Interface Sci. 265 (2003) 257–264.
[8] A.K. Jain, V.K. Gupta, A. Bhatnagar, Suhas, Utilization of industrial waste products as adsorbents for the removal of dyes, J. Hazard. Mater. 101 (2003) 31–42.
[9] V.K. Gupta, I. Ali, V.K. Saini, T. Van Gerven, B. Van der Bruggen, C. Vandecasteele, Removal of dyes from wastewater using bottom ash, Ind. Eng. Chem. Res. 44 (2005) 655–3664.
[10] V.K. Gupta, D. Mohan, V.K. Saini, Studies on the interaction of some azo dyes (naphthol red-J and direct orange) with nontronite mineral, J. Colloid Interface Sci. 298 (2006) 79–86.

[11] G. Lagaly, Bentonites: adsorbents of toxic substances, Prog. Colloid Polym. Sci. 95 (1994) 61–72.
[12] B.C. Qu, J.T. Zhou, X.M. Xiang, C.L. Zheng, H.X. Zhao, X.B. Zhou, Adsorption behavior of Azo Dye C.I. Acid Red 14 in aqueous solution on surface soils, J. Environ. Sci. 20 (2008) 704–709.
[13] L. Wang, A. Wang, Adsorption properties of Congo Red from aqueous solution onto surfactant-modified montmorillonite, J. Hazard. Mater. 160 (2008) 173–180.
[14] D. Ghosh, K.G. Bhattacharyya, Adsorption of methylene blue on kaolinite, Appl. Clay Sci. 20 (2002) 295–300.
[15] V. Ramasamy, K. Anandalakshmi, The determination of kaolinite clay content in limestones of western Tamil Nadu by methylene blue adsorption using UV–vis spectroscopy, Spectrochim. Acta A 70 (2008) 25–29.
[16] A.M. Li, M.J. Xu, W.H. Li, X.J. Wang, J.Y. Dai, Adsorption characterizations of fulvic acid fractions onto kaolinite, J. Environ. Sci. 20 (2008) 528–535.
[17] Y.M. Slokar, A.M. Le Marechal, Methods of decoloration of textile wastewaters, Dyes Pigments 37 (1997) 335–356.
[18] M.N.V.R. Kumar, T.R. Sridhari, K.D. Bhavani, P.K. Dutta, Trends in color removal from textile mill effluents, Colorage 40 (1998) 25–34.
[19] Y. Yukselen, A. Kaya, Suitability of the methylene blue test for surface area, cation exchange capacity and swell potential determination of clayey soils, Eng. Geol. 102 (2008) 38–45.
[20] P.T. Hang, G.W. Brindley, Methylene blue absorption by clay minerals. Determination of surface areas and cation exchange capacities (clay-organic studies XVIII), Clay Clay Miner. 18 (1970) 203–212.
[21] S.D.J. Inglethorpe, D.J. Morgan, D.E. Highley, A.J. Bloodworth, Industrial Mineral Laboratory Manual. Bentonite. Techinical Report WG/93/20. Mineralogy and Petrology Series, Br. Geol. Surv. (1993) 116.
[22] Y.S. Ho, G. McKay, Pseudo-second order model for sorption processes, Process Biochem. 34 (1999) 451–465.
[23] M. Kithome, J.W. Paul, L.M. Lavkulich, A.A. Bomke, Kinetics of ammonium adsorption and desorption by the natural zeolite clinoptilolite, Soil Sci. Soc. Am. J. 62 (1988) 622–629.
[24] J.R. Anderson, Y.-F. Chang, R.J. Western, Formation of phenazine from azobenzene over H-ZSM5: reaction control by a molecular constrained environment, Catal. Lett. 6 (1990) 59–66.
[25] J.A. Miwa, S. Weigelt, H. Gersen, F. Besenbacher, F. Rosei, T.R. Linderoth, Azobenzene on Cu(1 1 0): adsorption site-dependent diffusion, J. Am. Chem. Soc. 128 (2006) 3164– 3165.
[26] Z. Li, L. Gallus, Surface configuration of sorbed hexadecyltrimethylammonium on kaolinite as indicated by surfactant and counterion sorption, cation desorption, and FTIR, Colloids Surf. A: Physicochem. Eng. Aspects 264 (2005) 61–67.
[27] K.S. Low, C.K. Lee, Quaternized rice husk as sorbent for reactive dyes, J. Bioresour. Technol. 61 (1997) 121–125.
[28] A. Plemenschikov, J. Leszczynski, Adsorption of 1,3,5-trinitrobenzene on the siloxane sites of clay minerals: abinitio calculations of molecular models, J. Phys. Chem. B 103 (1999) 6886–6890.
[29] J.E. Gardolinski, L.P. Ramos, G.P. de Souza, F. Wypych, Intercalation of benzamide into kaolinite, J. Colloid Interface Sci. 221 (2000) 284–290.
[30] R. Takenawa, Y. Komori, S. Hayashi, J. Kawamata, K. Kuroda, Intercalation of nitroanilines into kaolinite and second harmonic generation, Chem. Mater. 13 (2001) 3741–3746.
[31] T.A. Elbokl, C. Detellier, Intercalation of cyclic imides in kaolinite, J. Colloid Interface Sci. 323 (2008) 338–348.
[32] B. Zhang, Y.F. Li, X.B. Pan, X. Jia, X.L. Wang, Intercalation of acrylic acid and sodium acrylate into kaolinite and their in situ polymerization, J. Phys. Chem. Solids 68 (2007) 135–142.
[33] D.R. Armstrong, J. Clarkson, W.E. Smith, Vibrational analysis of trans-azobenzene, J. Phys. Chem. 99 (1995) 17825–17831.
[34] N. Biswas, S. Umapathy, Structures, vibrational frequencies, and normal modes of substituted azo dyes: infrared, Raman, and density functional calculations, J. Phys. Chem. A 104 (2000) 2734–2745.
[35] K.M. Spark, R.S. Swift, Effect of soil composition and dissolved organic matter on pesticide sorption, J. Sci. Total Environ. 298 (2002) 147–161.